Fermi National Accelerator Laboratory

FERMILAB-Pub-78/72-EXP
7120.069

(Submitted to Phys. Rev. D)

MEASUREMENT OF MULTIPLE SCATTERING AT FERMILAB ENERGIES

G. Shen, C. Ankenbrandt, M. Atac, R. Brown, S. Ecklund,
P. J. Gollon, J. Lach, J. MacLachlan, and A. Roberts
Fermi National Accelerator Laboratory, Batavia, Illinois 60510

and

L. A. Fajardo, R. Majka, J. N. Marx, P. Nemethy, L. Rosselet,
J. Sandweiss, A. Schiz, and A. J. Slaughter
Yale University, New Haven, Connecticut 06520

October 1978

FERMILAB-Pub-78/72-EXP
Revised
May 15, 1979

MEASUREMENT OF MULTIPLE SCATTERING AT 50 TO 200 GeV/c

G. Shen, C. Ankenbrandt, M. Atac, R. Brown,* S. Ecklund,
P. J. Gollon, J. Lach, J. MacLachlan, and A. Roberts
Fermi National Accelerator Laboratory
Batavia, Illinois 60510

and

L. A. Fajardo, R. Majka,† J. N. Marx,† P. Nemethy,† L. Rosselet,
J. Sandweiss, A. Schiz, and A. J. Slaughter
Yale University
New Haven, Connecticut 06520

Multiple scattering distributions were measured at Fermilab energies with various targets from hydrogen to lead. Results are presented and compared with predictions of Moliere, Mayes et al., and Highland.

INTRODUCTION

Multiple Coulomb scattering of charged particles in matter is described by a number of theoretical treatments, with those of Moliere[1,2] and Nigam-Sundaresan-Wu[3] (NSW) being the most familiar. The various theories differ mainly in their treatment of the single scattering law. The Rutherford approximation should be altered to include screening and scattering by atomic electrons, relativistic and quantum effects, target recoil, and nuclear scattering. The NSW method uses the second Born approximation to a screened exponential potential for the single scattering law. The Moliere method is independent of the exact form of the single scattering law, but contains a model-dependent parameter representing the atomic screening. Since the two methods agree closely,[4] we shall not consider the NSW method in our comparisons.

Moliere calculates his screening parameter by using the Thomas-Fermi potential with the WKB method. Calculations by Tsai[5] show that this potential adequately describes the atomic screening for elements with atomic charge $Z \geq 5$. For higher Z elements, the 1/e angles (the scattering angles at which the distributions fall by 1/e) predicted by Moliere are consistent with previous experimental measurements.[6] Mayes et al.[6] find somewhat better agreement at lower Z if the Moliere screening parameter is modified empirically.

Yet to be resolved are disagreements in the tails of the distributions[7] and in the 1/e angles for low Z elements.[6] Data for

$Z \leq 5$ presently exist only for lithium and beryllium and then only with electron projectiles, for which scattering by atomic electrons has a significant effect. The lack of hydrogen data is surprising, considering its widespread use in high energy physics experiments. Finally, no published data exist above 600 MeV incident energy. (Present theories predict a factor of 1/p as the only momentum dependence, where p is the projectile momentum.)

In this paper we present measurements of the multiple scattering 1/e angles for incident pions, kaons, and protons at momenta of 70, 125, and 175 GeV/c on targets of beryllium, carbon, aluminum, copper, tin, and lead; and at momenta of 50 and 200 GeV/c on hydrogen. These angles are compared to the predictions of Moliere, Mayes et al. and to the Highland formula in "Review of Particle Properties."[8, 9]

APPARATUS

These data were taken as part of a Fermilab experiment to measure small angle scattering of pions, kaons, and protons by a variety of targets. The details of that experiment are described elsewhere.[10] For the purposes of this paper, only a portion of the apparatus is relevant.

The relevant apparatus, shown in Fig. 1, consisted of two proportional wire chambers (C) upstream of the target, and two similar chambers downstream. Each chamber contained planes in x and y (horizontal and vertical axes perpendicular to the beamline) with an effective wire spacing of 0.2 mm. The rms resolution of the

projected scattering angle is 26 μrad. Three upstream Cerenkov counters identified the incident particle. The momentum width ($\Delta p/p$) of the incident beam was less than 1.0% FWHM.

The trigger simply required the combination of scintillation counters $B_1B_2 \cdot (\overline{VH1})$ (Fig. 1) along with other beam-defining counters (not shown) much further upstream, and a Cerenkov signal. Off-line, an event was required to have one and only one hit per chamber plane.

ANALYSIS

The proportional chambers give the incoming and outgoing directions of the incident particle, and hence the scattering angle. The chamber wires effectively quantize the track angles, producing undesirable structure in the scattering angle distribution when projected along x or y. To reduce this effect, we choose to use the unprojected scattering angle distribution. The reasonable chi squares of our fits support this choice.

A potential problem in measuring the width of the unprojected angle distribution is the importance of correct chamber alignment; the distribution must be symmetric about the incident direction. This potential problem is eliminated by considering <u>differences</u> between consecutive events rather than each event singly. Thus for each chamber plane, the experimental quantities of interest are the coordinate differences between consecutive events instead of the coordinates themselves.[11]

In a single event, the chamber coordinates are ordinarily used in a straightforward way to determine the scattering angle, which for small angles can be represented by a two-dimensional vector

$$\vec{\theta} = (\theta_x, \theta_y). \tag{1}$$

If one follows the same procedure using coordinate differences instead, the result will be the vector difference between consecutive scattering angles. Thus, if we denote the event number by a subscript,

$$\vec{\phi}_i = \vec{\theta}_{i+1} - \vec{\theta}_i. \tag{2}$$

While $\vec{\phi}$ is the vector difference between scatters by the target in successive events, we can imagine the two scatters as occurring in a single event by two identical targets. The scatters are symmetric about the origin, so the vector sum of the scatters will have the same distribution as the vector difference. Thus, for multiple scattering by a target of thickness ℓ, if θ has a distribution $f(\theta, \ell)$ then ϕ will have the distribution $f(\phi, 2\ell)$. In sum, the experimental distributions obtained by considering differences between consecutive events should be compared with theoretical predictions corresponding to targets that are twice the actual thicknesses.

For the target thicknesses in this experiment, the Moliere distribution is well approximated by the three-parameter function[12]

$$\frac{d\sigma}{d\Omega} = \exp\left[A - (1+C)\ (\theta^2/\theta_e^2) + C\ (\theta^4/\theta_e^4)\right] \qquad (3)$$

for angles up to $2\theta_e$, where θ_e is the 1/e angle. This function is folded, at each momentum, with the angular distribution obtained with the target removed. The parameters are then adjusted to give the best fit between the result of the convolution and the distributions observed with the various targets. This procedure, effectively an empty-target subtraction, removes effects of angular resolution and scattering outside the target. Typical fits (for hydrogen and lead) are shown in Fig. 2.

Allowing all three parameters to vary gives a best-fit value for C that is consistent with the Moliere prediction.[13] However, the presence of local minima makes it difficult for the minimizing program (MINUIT) to find the best fit without occasional external guidance. Since the standard error of C is large (comparable to the value of C), and since the best fit value is consistent with theory, we choose to fix C at its predicted value in our fits to determine θ_e. These predicted values of C are given in Table I.

RESULTS AND CONCLUSIONS

Properties of the targets used in this experiment are presented in Table I. Twice the actual thickness is about 0.1 radiation length in all cases.

The ratio, R, of the fitted θ_e values to the Moliere prediction for the various targets and projectiles is presented in

Table II. As expected, we observe no statistically significant difference due to projectile type. To quantify this, we compute the quantity

$$D_{ab} = (R_a - R_b)/(R_a + R_b) \qquad (4)$$

for projectiles a and b at each momentum, combining the results from the various targets. The results, presented in Table III, show D_{ab} is consistent with being zero for projectiles of different type. We are then justified in consolidating data with different projectile types. The consolidated results[14] are presented in Table IV. Inspection of Table IV reveals no momentum dependence, so we further consolidate results from different momenta in Table V and Fig. 3.

The tables and Fig. 3 contain statistical errors only. We estimate the systematic error (mainly from the uncertainty of the beam momentum) to be less than 0.4%.

Three experiment-theory ratios are presented in Tables IV and V. Along with the Moliere prediction of the 1/e angle, we also try the empirical adjustment to the Moliere theory given by Mayes et al.[6] and the formula by Highland. The Moliere prediction is obtained from equations 22 and 25 of Ref. 2. For the Highland formula, we took

$$\theta_e = \frac{17.5}{p}\sqrt{\frac{L}{L_R}}\left[1 + 0.125 \log_{10}\left(\frac{L}{0.1\ L_R}\right)\right]$$

$$= \frac{19.7}{p}\sqrt{\frac{L}{L_R}}\left[1 + \frac{1}{9}\log_{10}\left(\frac{L}{L_R}\right)\right], \qquad (5)$$

where p is the projectile momentum in MeV/c, L/L_R is the length of the target in radiation lengths, and θ_e is the 1/e multiple scattering angle in radians. The numerical constants in Eq. 5 were chosen by Highland in order to agree with Moliere in the domain of high Z and $0.001 < L/L_R < 10$.

The Moliere prediction is in excellent agreement with the data. Although the Thomas-Fermi potential is not expected to be applicable at very low Z, we find excellent agreement even for hydrogen.

The Highland formula is in poorest agreement with hydrogen, although it is within his stated uncertainty of 20%. In the Highland formula, the target dependence enters by way of the radiation length, instead of a model-dependent function of Z as in the case of Moliere. Two targets having the same radiation length will produce equal scatteirng widths, independent of Z. At low Z, the Highland relationship between multiple scattering and radiation length might still be expected to hold. The disagreement of our hydrogen measurement with Highland, however, suggests either that this relationship does not hold at low Z, or that the value for the hydrogen radiation length is not correct.

The radiation lengths used were taken from "Review of Particle Properties" and were originally calculated by Tsai in Ref. 5. The radiation length for hydrogen is calculated using the atomic wave function. The molecular wave function yields a shorter radiation length[15] which increases the disagreement.

We find good agreement with all theories for the high Z targets.

The current "Review of Particle Properties"[16] has replaced the Highland formula with

$$\theta_{\text{plane}}^{\text{rms}} = \frac{15}{P}\sqrt{\frac{L}{L_R}}(1+\varepsilon), \tag{6}$$

or equivalently

$$\theta_e = \sqrt{2}\,\theta_{\text{plane}}^{\text{rms}} = \frac{21.2}{P}\sqrt{\frac{L}{L_R}}(1+\varepsilon). \tag{7}$$

If we set $\varepsilon = 0$ (where Eqs. 6 and 7 reduce to the Rossi-Greisen formula[17]), we get values for $\theta_{exp}/\theta_{theory}$ of about 0.8 at high Z and 0.74 for hydrogen.

We emphasize that our results represent a test of standard multiple scattering formulations in the domain of extremely relativistic, non-electron projectiles, and for $L/L_R \simeq 0.1$.

ACKNOWLEDGEMENTS

We are grateful to Dr. K. Hanson for a number of useful conversations. This work was supported in part by the U.S. Department of Energy. One of us (L.R.) was a fellow of the Swiss National Fund for Scientific Research and a second member (LAF) was supported in part by a Ford Foundation Fellowship for Mexican-Americans and Puerto Ricans.

REFERENCES

*Visitor from Rutherford Laboratory, Chilton, Didcot, Berkshire, England.

†Present address: Lawrence Berkeley Laboratory, Berkeley, California 94720.

[1]G. Moliere, Z. Naturforsch. 2a, 133 (1947); 3a, 78 (1948).

[2]H. A. Bethe, Phys. Rev. 89, 1256 (1953).

[3]B. P. Nigam, M. K. Sundaresan, and T. Y. Wu, Phys. Rev. 115, 491, (1959).

[4]J. B. Marion and B. A. Zimmerman, Nucl. Instrum. Methods 51, 93 (1967).

[5]Y. S. Tsai, Rev. Mod. Phys. 46, 815 (1974).

[6]B. W. Mayes et al., Nucl. Phys. A230, 515 (1974).

[7]E. V. Hungerford et al., Nucl. Phys. A197, 515 (1972).

[8]Particle Data Group, Rev. Mod. Phys. 48, No. 2, Part II (1976); Erratum in Phys. Lett. 68B, 1 (1977).

[9]V. L. Highland, Nucl. Instrum. Methods 129, 497 (1975). The center-of-mass correction factor is incorrect. No such correction is necessary to first order, even non-relativistically. (Virgil Highland, private communication.)

[10]A. J. Slaughter et al., "A High Resolution Spectrometer for a Small Angle Scattering Experiment at Fermilab", in preparation.

[11]Since each event contributes to two event differences, a correlation is introduced into the data distributions. The effect is an increase in the uncertainty of θ_e by a factor of $\sqrt{3/2}$ over the uncorrelated uncertainty.

[12] The distribution is nearly Gaussian for Θ less than Θ_e (C is small). The third term on the right is the next term in the expansion in Θ^2, which is included to describe the non-gaussian tail.

[13] The Moliere distribution is set equal to the right side of Eq. 3 at $\Theta = 0$, $\chi_c\sqrt{B}$, and $2\chi_c\sqrt{B}$ (using the variables of Ref. 2). We then solve the three equations for the three parameters.

[14] The consolidation is done by combining histograms of the data and performing a separate fit. Since the combined histograms have more data, a larger number of bins can be included in the consolidated fit, giving greater statistical accuracy.

[15] D. Bernstein and W. K. H. Panofsky, Phys. Rev. 102, 522 (1956).

[16] Particle Data Group, Phys. Lett. 75B, No. 1 (1978).

[17] B. Rossi and K. Greisen, Rev. Mod. Phys. 13, 240 (1941).

FIGURE CAPTIONS

Figure 1: Plan view of the experiment. The proportional wire chambers are labeled C. B_1, B_2, and VH1 are scintillation counters, with a 3 cm square hole in the center of VH1.

Figure 2: Typical θ^2 distributions. The top distributions were obtained with the indicated targets and momenta, while the lower ones were obtained with the targets removed. The solid curves are the best fitting convolutions of the lower distributions with Eq. 3. The dashed lines serve only to guide the eye.

(a) 70 GeV/c negative projectiles on lead.
χ^2 = 17.7 for 18 degrees of freedom.

(b) 50 GeV/c negative projectiles on hydrogen.
χ^2 = 30.6 for 18 degrees of freedom.

Figure 3: Comparison of experimental 1/e angle with the predictions of Moliere, Mayes et al. and Highland, as a function of Z. Experimental error bars are shown only for the Moliere comparison since the fractional error at each Z is the same in all cases.

TABLE I

Target characteristics. The projectile momentum is p. The values of C and $p\theta_e$ are for targets twice the actual thicknesses.

Target	L/L_R	C	Predicted $p\theta_e$ (MeV/c)		
			Moliere	Mayes	Highland
H	0.0589	0.0356	5.46	5.61	6.06
Be	0.0454	0.0372	4.93	5.07	5.25
C	0.0482	0.0374	5.12	5.27	5.43
Al	0.0450	0.0387	5.02	5.17	5.22
Cu	0.0554	0.0397	5.70	5.86	5.86
Sn	0.0693	0.0406	6.52	6.67	6.63
Pb	0.0454	0.0443	5.21	5.31	5.25

TABLE II

The ratio $R = \theta_{exp}/\theta_{Moliere}$ for each target and projectile type and momentum. θ_{exp} and $\theta_{Moliere}$ are the experimental and Moliere-predicted 1/e angles.

Projectile Momentum (GeV/c)	Target	Projectile					
		π^+	π^-	K^+	K^-	p	$\bar{p}$
50	H	1.007±.016	0.947±.013	0.99±.04	1.01±.06	0.997±.018	0.97±.05
70	Be	1.08±.12	1.05±.11	1.09±.15	1.06±.13	0.99±.12	
70	C	1.00±.09	1.11±.12	0.99±.13	1.01±.18	1.02±.13	
70	Al	1.04±.07	0.98±.09	0.91±.10	1.04±.07	1.02±.07	1.04±.12
70	Cu	0.96±.06	0.96±.09	1.00±.08	0.95±.08	1.06±.07	0.98±.13
70	Sn	1.02±.05	0.95±.06	1.00±.07	1.01±.05	1.01±.06	1.04±.08
70	Pb	0.88±.06	1.01±.07	0.92±.08	1.01±.06	1.05±.06	1.03±.11
125	Be	1.07±.29		1.06±.54		0.67±.35	
125	Al	1.02±.22		0.99±.43		0.98±.20	
125	Pb	1.04±.18		1.02±.38		0.90±.18	
175	Be	1.13±.38	1.13±.13	1.00±.44	0.63±.40	1.31±.22	
175	C	0.91±.31	0.96±.14		1.04±.25	1.01±.19	
175	Al	0.67±.39	0.96±.12	0.62±.64	0.74±.28	0.95±.19	
175	Cu	0.99±.19	1.15±.13	0.97±.27	1.03±.24	1.11±.12	
175	Sn	0.98±.16	0.82±.12	0.87±.24	0.80±.18	0.92±.11	
175	Pb	0.89±.23	0.92±.11	0.84±.32	0.99±.18	1.01±.14	
200	H	1.03±.10	1.05±.08	0.95±.14	1.04±.15	0.94±.12	1.36±.27

TABLE III

The quantity $D_{ab} = (R_a - R_b)/(R_a + R_b)$ for projectiles a and b. Values of D from the various targets available at each momentum (see Table II) are consolidated. In addition, projectile charges are consolidated for the first three rows and projectile species are consolidated for the final row.

a	b	50 GeV/c	70 GeV/c	175 GeV/c	200 GeV/c
π	K	-0.007±.018	-0.006±.053	0.05±.17	0.024±.061
π	p	0.001±.011	-0.052±.049	-0.08±.22	-0.019±.065
p	K	-0.003±.020	0.049±.056	0.15±.28	0.054±.077
+	-	0.009±.008	0.002±0.36	-0.03±.10	0.000±.042

TABLE IV

The ratio $\theta_{exp}/\theta_{theory}$ after consolidating data with different projectile types.

Projectile Momentum (GeV/c)	Target	$\theta_{exp}/\theta_{theory}$		
		Moliere	Mayes	Highland
50	H	0.993±.008	0.966±.008	0.894±.007
70	Be	1.00±.04	0.97±.04	0.94±.04
70	C	1.06±.04	1.03±.04	1.00±.04
70	Al	1.02±.03	0.99±.03	0.98±.03
70	Cu	0.98±.03	0.95±.03	0.95±.03
70	Sn	1.03±.02	1.00±.02	1.01±.02
70	Pb	0.99±.02	0.97±.02	0.98±.02
125	Be	0.99±.12	0.96±.12	0.93±.11
125	Al	0.97±.10	0.94±.09	0.94±.09
125	Pb	0.99±.08	0.97±.08	0.98±.08
175	Be	1.09±.08	1.06±.08	1.02±.08
175	C	0.90±.09	0.87±.08	0.84±.08
175	Al	0.96±.07	0.94±.07	0.93±.07
175	Cu	1.04±.06	1.01±.06	1.01±.06
175	Sn	0.92±.05	0.90±.05	0.91±.05
175	Pb	0.92±.06	0.90±.06	0.91±.06
200	H	1.04±.04	1.01±.04	0.94±.04

TABLE V

The ratio $\Theta_{exp}/\Theta_{theory}$ after consolidating data with different projectile types and momenta.

Target	Z	$\Theta_{exp}/\Theta_{theory}$		
		Moliere	Mayes	Highland
H	1	0.993±.008	0.966±.008	0.894±.007
Be	4	1.018±.037	0.989±.036	0.955±.035
C	6	1.026±.040	0.997±.039	0.968±.037
Al	13	1.008±.027	0.979±.026	0.970±.026
Cu	29	0.991±.027	0.963±.027	0.965±.027
Sn	50	1.010±.021	0.986±.020	0.991±.020
Pb	82	0.981±.022	0.962±.022	0.975±.022

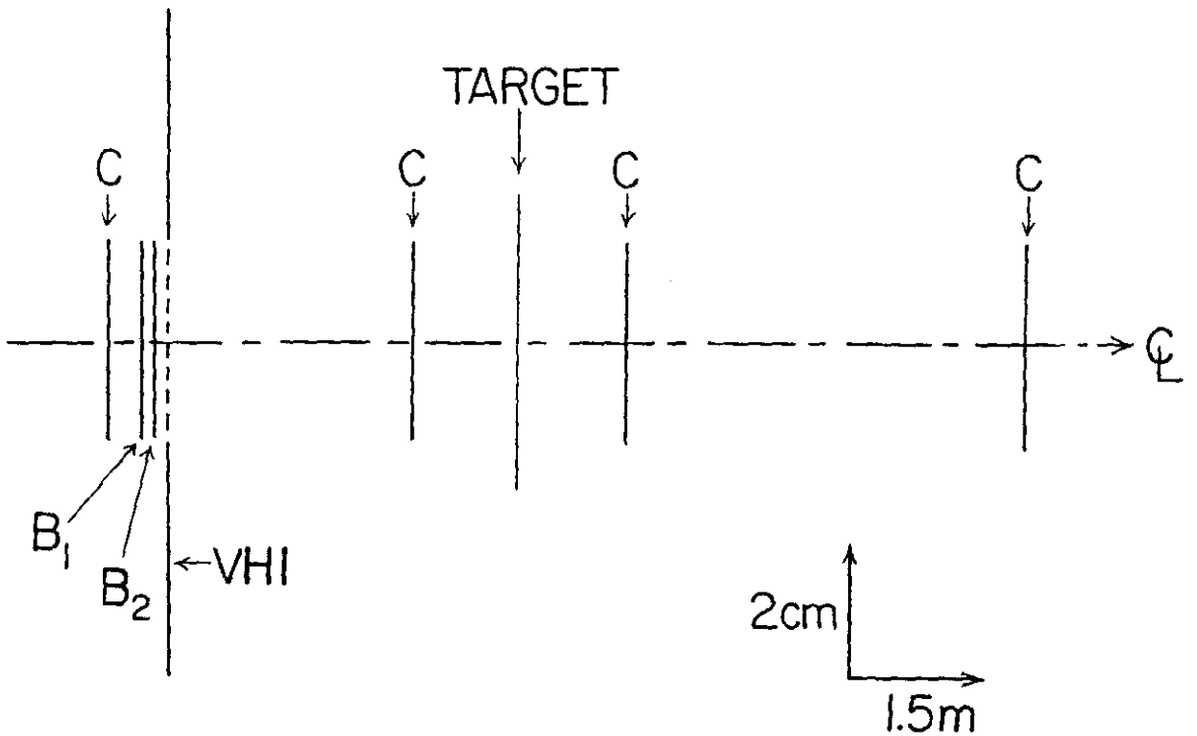

Figure 1

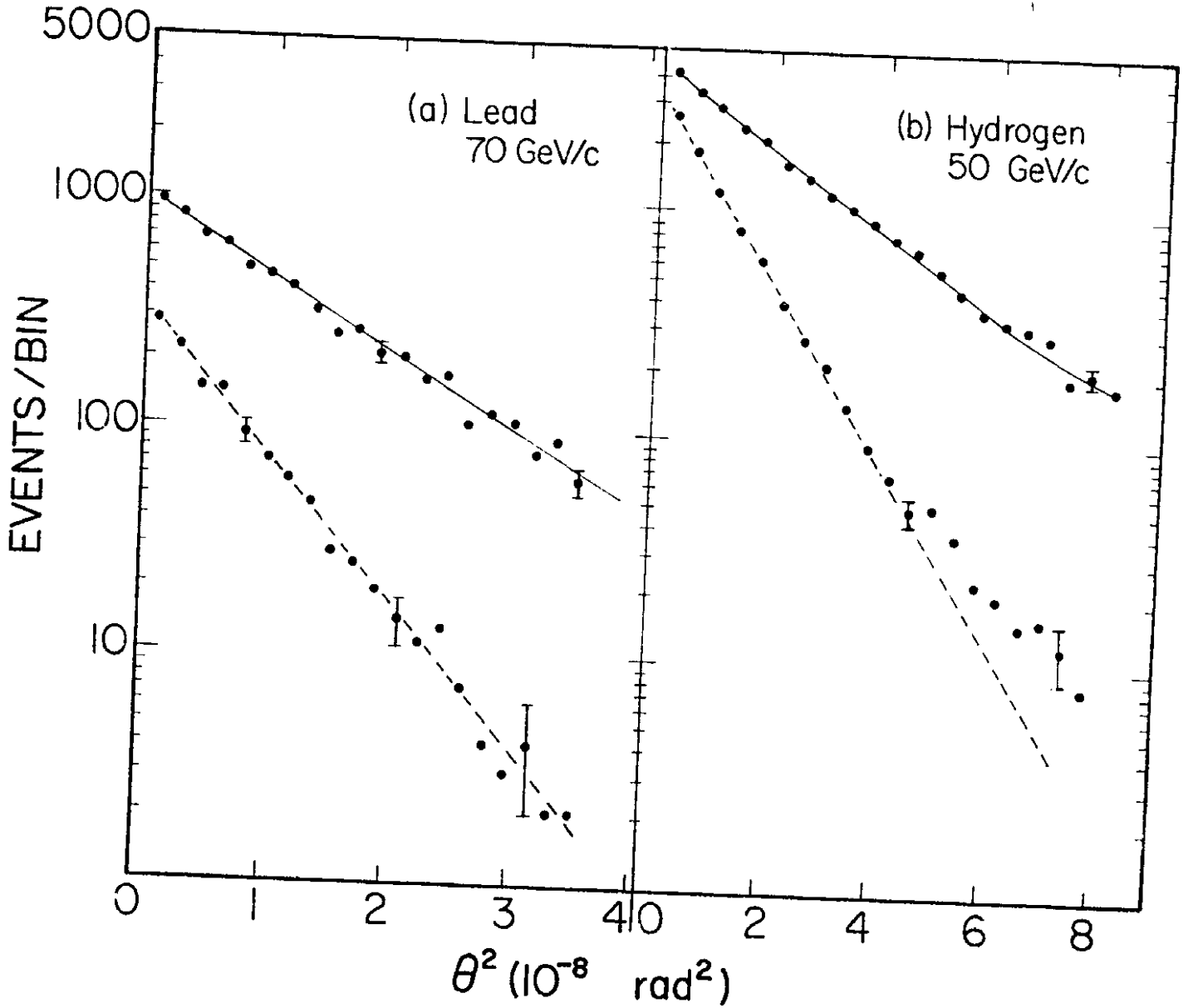
5000
1000
100
10
EVENTS/BIN
(a) Lead
70 GeV/c
(b) Hydrogen
50 GeV/c
0
1
2
3
4
0
2
4
6
8
θ² (10⁻⁸ rad²)

Figure 2

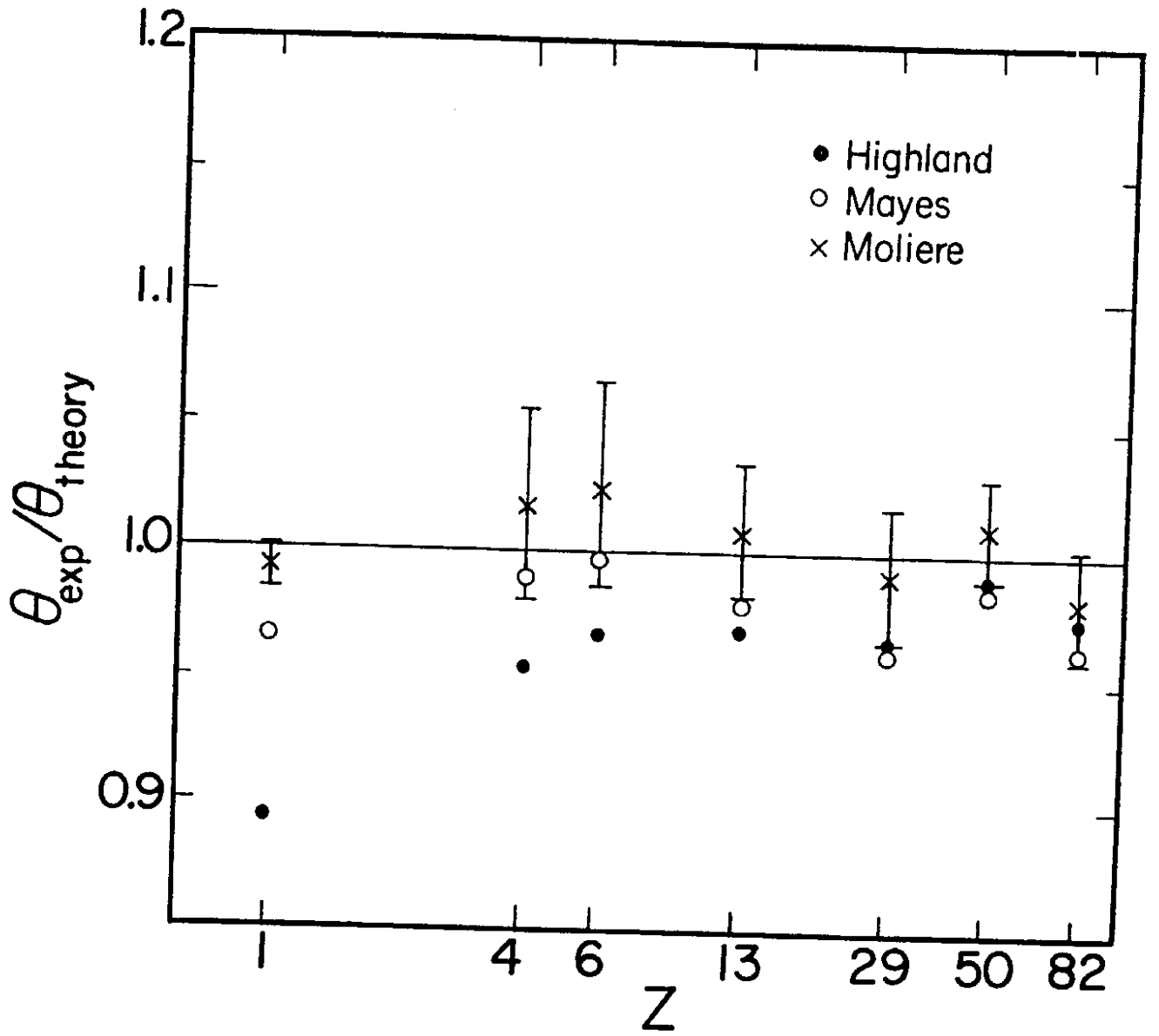
1.2
1.1
1.0
0.9
$\theta_{exp}/\theta_{theory}$
Highland
Mayes
Moliere
1
4
6
13
29
50
82
Z

Figure 3